ЖУРНАЛ СТРУКТУРНОЙ ХИМИИ

2014. Том 55, № 4 *Июль – август* *С. 648 – 655*

UDC 541.6:546.59:546.621

STRUCTURES, STABILITIES, AND ELECTRONIC PROPERTIES OF Al_nAu (n = 1—15) CLUSTERS: A DENSITY FUNCTIONAL STUDY

S.Y. Li, L. Guo, R.J. Zhang, X. Zhang

School of Chemistry and Material Science, Shanxi Normal University, Linfen, China
E-mail: gl-guoling@163.com

Received January, 25, 2013 *Revised — March, 11, 2013*

We present density functional calculations of Al_nAu clusters for n = 1—15. The growth pattern for Al_nAu (n = 1—7, 12, 14, 15) clusters is the Au atom occupying a peripheral position of Al_n clusters, and the growth pattern for Al_nAu (n = 8, 10 and 13) clusters is Au-substituted Al_{n+1} clusters. It is found that the Au atom replaces the surface atom of an Al_{n+1} cluster and occupies a peripheral position. In addition, the ground state structures of Al_nAu clusters are more stable than pure Al_n clusters. It is found that the $Al_{13}Au$ cluster exhibits high stability.

K e y w o r d s: Al_nAu bimetallic clusters, DFT calculations, relative stability, electronic structure.

INTRODUCTION

Clusters exhibit many interesting properties that are neither atomic-like nor extended solid-like. It is expected that materials assemblies from finite-sized clusters have many special properties. Thus, much attention has been paid to the study of atomic clusters from both theoretical and experimental sides during the last few years [1, 2]. In recent years, a number of series of experimental and theoretical works have been devoted to the studies of transition metal doped Al clusters, such as Al_nMg [3], Al_nZn [4], Al_nFe [5], Al_nCo [6], Al_nCu [7, 8] and so on [9, 10]. Furthermore, gold-containing bimetallic clusters are significant due to their special technical applications in the fields of optics, materials science, catalysis, and solid state chemistry [11—21]. Especially, Al—Au alloy clusters have been reported [12—14, 21]. It is known that pure Al_{13} has 39 valence electrons. Doping of Al_{13} cluster with a gold atom leads to the required ″magic″ number of valence electrons for shell closure. This is in line with the spherical jellium model (SJM). The SJM predicts that the clusters with 2, 8, 20, 40 … valence electrons have higher stability due to the closure of electronic shells [22, 23].

In this work, we investigate the relative ordering of these structures with the Au impurity occupying the internal and other position. Here, we study the evolution of the binding energy, dissociation energy, HOMO—LUMO gap, ionization potential, electron affinity, and hardness for Al_nAu (n = 1—15) clusters. These physical values are compared with their counterparts calculated at the same level for pure aluminum clusters.

In the following section, we briefly outline the computational methodology. Then the results are presented and discussed, and we give some conclusions in the end.

METHODOLOGY AND COMPUTATIONAL DETAILS

All of the calculations are carried out with the Gaussian-03 program package [5, 24]. The geometrical parameters for several different starting structures were optimized completely using the density functional theory selecting Becke′s three-parameter hybrid exchange functional [25] in combination

Table 1

Calculated bond lengths, averaged binding energies, and vertical ionization potentials, experiment results, and theoretical results of this work

Parameter	Au_2		Al_2		AlAu	
	This work	Experimental[30]	This work	Experimental[31]	This work	Experimental[32]
Bond length, Å	2.573	2.472	2.514	2.560	2.414	2.339
Ionization potential, eV	9.426	9.200±0.210	6.294	6.200±0.200	7.992	5.96±0.04
E_b, eV	1.864	2.290±0.100	0.585	0.997±0.108	1.577	1.670±0.009

with the Lee-Yang-Parr correlation functional (B3LYP) method. An all-electron basis set 6-31G* is used for the Al atom. The LANL2DZ pseudopotential is adopted for the valence electrons of the Au atom, and its core electrons are represented by the LANL2DZ effective core potential (ECP) [26—28]. This scheme is a good compromise between accuracy and computational effort, and its application has been shown to be effective for many species including transition atom such as Au_nCs systems [19].

The selection of distinct initial geometries is important for the reliability of the ground state structures obtained. As the cluster size increases, the number of possible geometries increases dramatically. In this paper, the conformations of pure Al_n clusters are obtained firstly by reference to the configurations in [3, 29]. The geometries with different symmetries are also optimized for each size. During the course of choosing the initial structures of Al_nAu clusters, we have considered possible isomeric structures by placing the Au atom on each possible site of the Al_n cluster as well as by substituting one Al atom by the Au atom from the Al_{n+1} cluster. The Al_nMg [3], Al_nZn [4], Al_nFe [5], and Al_nCu [7] stable isomers are also considered as candidates. For all isomers of each cluster, the local minima of the potential energy surface are guaranteed by the harmonic vibrational frequencies without imaginary modes. Further, different spin multiplicities of the low-lying energy isomers are considered.

In order to test the reliability of our calculation, the Au_2, Al_2, and AlAu dimers are calculated. The results are summarized in Table 1. As illustrated in Table 1, our results are in good agreement with previous experimental and theoretical data.

RESULTS AND DISCUSSION

Equilibrium structures of neutral Al_{n+1} AND Al_nAu (n = 1—15) clusters. In cluster physics, one of the most fundamental problems is to determine the ground state geometry. Firstly, we study the ground state structures of Al_nAu clusters. The ground state configurations of Al_nAu (n = 1—15) clusters and some low-lying energy states are demonstrated in Fig. 1. For a proper comparison we have also shown the ground state configurations of pure Al_{n+1} (n = 1—15) clusters. The relative energy of a structural isomer from the ground state is also labeled below the structural plots. Meanwhile, we give a clear indication of the geometry symmetry and multiplicity of each isomer. The corresponding energy, symmetries (Sym), multiplicity(M), HOMO—LUMO gap (Gap), atomic averaged binding energy (E_b), the second-order energy differences (Δ_2E), vertical ionization potential (VIP), vertical electron affinities (VEA), and energies (E) (all in eV) for the most stable Al_nAu clusters are all shown in Table 2.

For small clusters containing up to 3 atoms, the structural characteristic of the lowest energy isomers is planar, which is in agreement with other studies. For the Al_1Au cluster with the $C_{\infty v}$ symmetry, the corresponding electronic state is $^1\Sigma g$. The Al—Au distance (2.414 Å) is shorter than that Al—Al distance (2.564 Å) of the Al_2 cluster, which is close to Belcher′s studies (2.36 Å) [11].

The doublet Al_2Au cluster, the lowest energy structure is an isosceles triangle (C_{2v}), in which the Au atom is at the apex, the Al—Al distance (2.665 Å) is longer than that of the Al_2 (2.564 Å) cluster, which is close to Belcher′s studies (2.68 Å) [11]. The Al—Au bond length is 2.508 Å. The bond angle of Al—Au—Al atoms is 64.19. The corresponding electronic state is $^2B_1$. The lowest energy structure

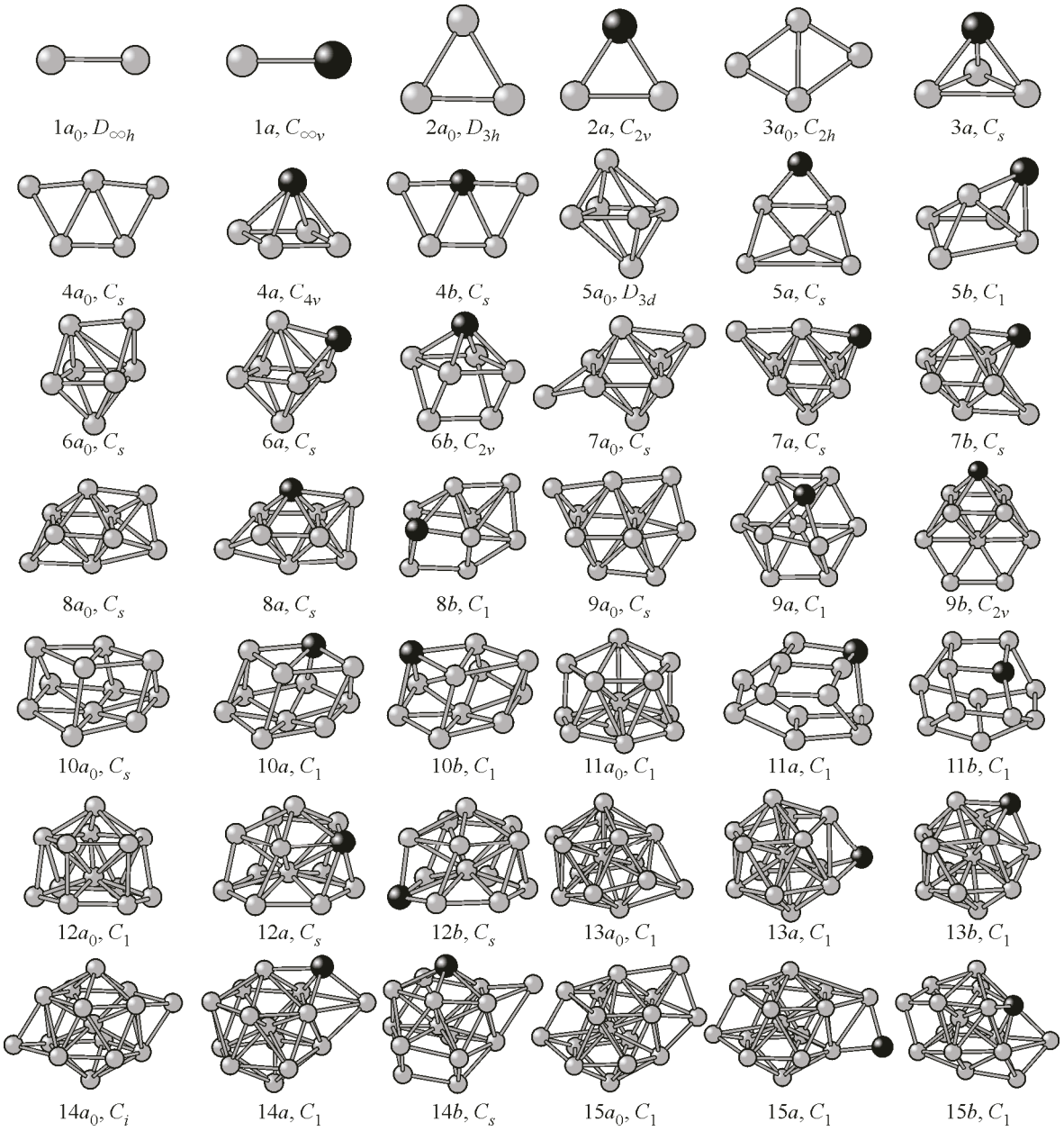

Fig. 1. Lowest-energy and low-lying structures of Al_nAu (n = 1—15) clusters and lowest-energy structures of Al_{n+1} (n = 1—15) clusters. The black and gray balls represent the Au and Al atoms respectively

of Al_3 is an equilateral triangle structure with the D_{3h} symmetry [29]. Al_2Au is generated by substituting one Au atom for one Al atom of the Al_3 cluster.

Al_3Au is the three-dimensional structure. It is pyramidal with the C_s symmetry, in which the Au atom sits on the hallow site of the triangular Al_3 cluster. The triplet isomer with the electronic state $^3A''$ is lower in total energy than the singlet isomer by 0.046 eV. Therefore, the spin triplet configuration is a more stable structure. However, Al_4 is a rhomboidal structure with the C_{2h} symmetry [3].

The Al_4Au cluster is a square pyramidal (C_{4v}) structure with a spin doublet as its ground state, in which the Au atom occupies the top position of Al_4. The corresponding electronic state is $^2A_1$. For Al_5, the most stable structure is a pentagon structure with the C_s symmetry. The low-lying isomer with the higher energy (0.294 eV) is similar to the Al_5 configuration, where the Au atom is at the pentagon vertex position.

Table 2

Multiplicity (M), *symmetries* (Sym), HOMO—LUMO *gap* (Gap), *averaged binding energy* (E_b), *dissociation energy* (ΔE), *second-order energy differences* ($\Delta_2 E$), *vertical ionization potential* (VIP), *vertical electron affinities* (VEA), *and energies* (E) (*all in* eV) *for the most stable* Al_nAu (n = 1—13) *clusters*

Cluster	M	Sym	Gap	E_b	ΔE	$\Delta_2 E$	VIP	VEA	E
Al_1Au	1	$C_{\infty v}$	3.506	1.577	—	—	7.992	0.539	–10283.838
Al_2Au	2	C_{2v}	1.205	1.464	1.239	–0.457	6.174	1.410	–16880.257
Al_3Au	3	C_s	1.385	1.522	1.696	–0.129	6.071	1.450	–23477.131
Al_4Au	2	C_{4v}	1.286	1.583	1.825	–0.020	6.272	1.913	–30074.135
Al_5Au	1	C_s	1.633	1.627	1.845	–0.734	6.280	1.831	–36671.160
Al_6Au	2	C_s	1.324	1.763	2.579	0.362	6.716	2.425	–43268.918
Al_7Au	1	C_s	1.788	1.819	2.217	0.488	6.308	1.660	–49866.314
Al_8Au	2	C_s	1.578	1.809	1.728	–0.648	6.193	2.250	–56463.222
Al_9Au	1	C_1	1.503	1.866	2.376	0.410	6.221	2.223	–63060.776
$Al_{10}Au$	2	C_1	1.457	1.875	1.966	–0.525	6.033	2.329	–69657.921
$Al_{11}Au$	1	C_1	1.772	1.926	2.491	0.172	6.193	2.035	–76255.592
$Al_{12}Au$	2	C_s	1.368	1.957	2.319	–0.987	6.123	2.577	–82853.088
$Al_{13}Au$	1	C_1	2.476	2.053	3.306	1.849	6.561	1.818	–89451.575
$Al_{14}Au$	2	C_1	1.656	2.013	1.457	–1.095	5.735	2.237	–96048.209
$Al_{15}Au$	1	C_1	1.697	2.047	2.552	—	6.030	2.098	–102645.940

For the spin singlet Al_5Au with the electronic state $^1A'$, the Al atom bridging the Al_5 pentagon [29] with the C_s symmetry is the lowest energy configuration. This structure is different from the Al_6 cluster which is a tetragonal bipyramid with the D_{3d} symmetry [4]. The low-lying isomer is a distorted prism structure with the C_1 (^1A) symmetry.

The lowest-energy isomer of Al_6Au is a spin doublet distorted capped triangular prism structure with the C_s (^2A) symmetry, which is capped by one Au atom on the Al_6 cluster. It is in accordance with the study of Michele L. et al. [14]. The low-lying isomer is a capped triangular prism structure with the C_{2v} ($^2A_1$) symmetry, above 0.065 eV in energy. Pure Al_7 adopted the distorted capped trigonal prism with the C_s symmetry.

For spin singlet Al_7Au with the electronic state ^1A, the most stable structure is obtained by capping one Au on the Al_7 cluster. Its symmetry is C_s. It is different from the Al_8 structure which is the distorted rhombic prism with the C_s symmetry.

The lowest energy structure for Al_8Au is spin doublet with the C_s ($^2A'$) symmetry, which can be seen as a substituting structure of the Al_9 cluster. The ground state geometry of Al_9 is one capped Al atom on the Al_8 cluster. However, the low-lying structure is completely different from the lowest energy structure.

The ground state geometry of the $Al_{10}Au$ cluster with C_1 symmetry can be seen as a substituting structure of the Al_{11} cluster. Another isomer 10b is also the Au atom substituting for Al in the Al_{11} cluster with the C_1 symmetry, higher by 0.086 eV than 10a. The most stable structure of Al_{11} develops pentagonal arrangements of the atoms.

The lowest energy structures for Al_nAu (n = 12—15) clusters are the spin doublet with C_s, the spin singlet with C_1, the spin doublet with C_1, the spin singlet with C_1 respectively. Among them, $Al_{12}Au$, $Al_{14}Au$, and $Al_{15}Au$ have the same growth pattern as Al_nAu (n = 1—7), while the growth pattern of $Al_{13}Au$ is the same as that of Al_8Au and $Al_{10}Au$. The ground state structure of Al_{14} can be obtained by capping one Al atom on the icosahedron with the C_1 symmetry. The lowest-energy structure of Al_{15} [3] is a bicapped icosahedron with the C_i symmetry.

In the case of the $Al_{12}Au$ cluster, we find that the ground state structure is the spin doublet geometry with the C_s symmetry, which is different from the Rajendra et al. [12] prediction. Our result is lower in total energy by 0.43 eV. Rajendra′s studies appeared to have established the ground state ge-

ometry of $Al_{13}Au$ to be the Au atom sitting inside the icosahedral-like cage of Al atoms. We give the different conclusion. The lowest energy isomer of $Al_{13}Au$ is a spin singlet with Au at the surface position, which is 0.38 eV lower in energy. We can also see that the Au impurities of $Al_{12}Au$ and $Al_{13}Au$ prefer to occupy the peripheral sites of Al_{12} and Al_{13} clusters.

In summary, the growth pattern for Al_nAu (n = 1—7, 12, 14, 15) clusters is the Au atom occupying a peripheral position of Al_n clusters [29]. The growth pattern for Al_nAu (n = 8, 10, 13) clusters is Au-substituted Al_{n+1} clusters. It is found that the Au atom replaces the surface atom of the Al_{n+1} cluster and occupies a peripheral position. The structures of Al_9Au and $Al_{11}Au$ do not meet the above rule.

STABILITIES AND ELECTRONIC PROPERTIES

We now discuss the relative stability of these clusters by computing the energy that is indicative of the stability. We compute the atomization or the binding energy (E_b) per atom, the dissociation energy (ΔE), and the second-order energy differences ($\Delta_2 E$) as, respectively,

$$E_b[Al_nAu] = (nE[Al] + E[Au] - E[Al_nAu])/(n + 1), \quad (1)$$

$$\Delta E[Al_nAu] = E[Al_{n-1}Au] + E[Al] - E[Al_nAu], \quad (2)$$

$$\Delta_2 E[Al_nAu] = E[Al_{n+1}Au] + [Al_{n-1}Au] - 2E[Al_nAu]. \quad (3)$$

In general, E_b increases sharply for a very small cluster and then a plateau follows as the cluster size grows. Small humps or dips for the specific size of clusters signify their relative stabilities. E_b of the Al_nAu cluster (Fig. 2) is calculated using Eq.(1), where E(Al), E(Au), and $E(Al_nAu)$ represent the energies of an Al atom, an Al atom, and the total energy of the Al_nAu cluster respectively. For comparison, we also plot E_b of the host Al_n cluster, $E_b[Al_n] = (nE[Al] - E[Al_nAu])/n$ (Fig. 2). As seen in this figure, the average binding energies of most Al_nAu clusters are higher than those of the pure Al_n clusters (except for n = 14). It indicates that the Au atom doped in the Al_n clusters contributes to strengthen the stabilities of the aluminum framework. For Al_nAu, E_b evolves monotonically with a total number of atoms in the cluster. Especially, for n = 2—7 E_b increases rapidly from 1.464 eV for Al_2Au to 2.059 eV for Al_7Au, which corresponds to the structure transition from two to three dimension. E_b increases gradually in the range n = 8—15, in which the rate of the increase becomes weak (only from 1.819 eV to 2.053 eV). In addition, the comparison of aluminum with the BE curve for Al_nAu clusters shows that small Al_nAu clusters are strongly bound. Especially, E_b of $Al_{13}Au$ (2.053 eV) is the highest one as compared to other clusters, which shows that the $Al_{13}Au$ structure is most stable among the Al_nAu clusters. As the cluster grows in size, the difference between the BE curve of Al_nAu clusters and pure aluminum clusters continue to diminish, indicating that the bonding in doped clusters is essentially similar to that in pure clusters.

In cluster physics, the dissociation energy (ΔE) and the second order energy differences ($\Delta_2 E$) are sensitive quantities that reflect the relative stability of the investigated clusters. ΔE shows the energy for one atom to be separated from the host clusters. $\Delta_2 E$ is often compared directly with the relative abundances determined in mass spectroscopy experiments. They are defined as Eqs. (2) and (3), where $E(Al_nAu)$, $E(Al_{n+1}Au)$, $E(Al_{n-1}Au)$, and E(Al) represent the total energies of the most stable Al_nAu, $Al_{n+1}Au$, and $Al_{n-1}Au$ clusters and an Al atom respectively. As shown in Fig. 3, particularly prominent maxima of $\Delta_2 E$ are found at n = 4, 6, 7, 9, 11, 13, indicating higher stability in comparison with their neighboring cluster. It is observed that, for the Al_nAu cluster, ΔE of Al_6Au (2.579 eV),

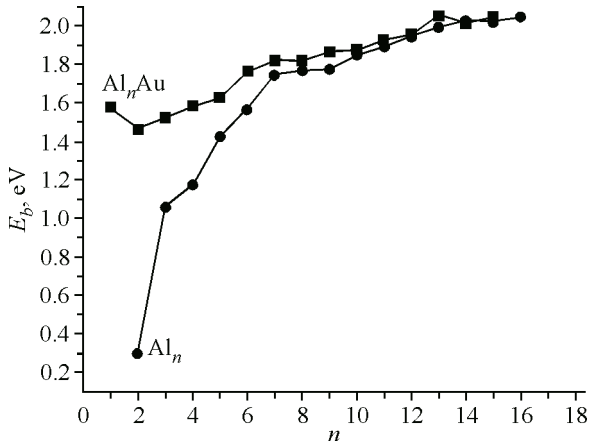

Fig. 2. Binding energy per atom of Al_nAu and Al_{n+1} clusters

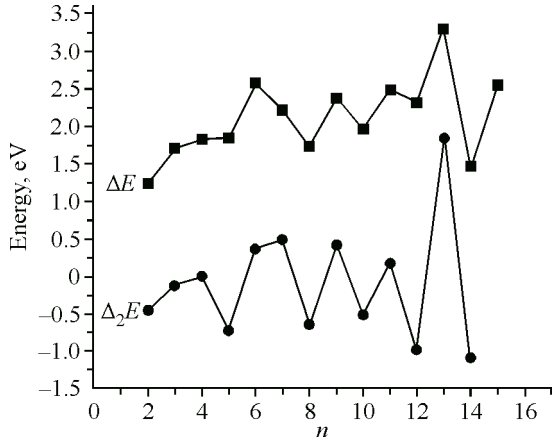

Fig. 3. Second-order energy difference Δ_2E and the dissociation energy of the Al_nAu (n = 1—15) clusters

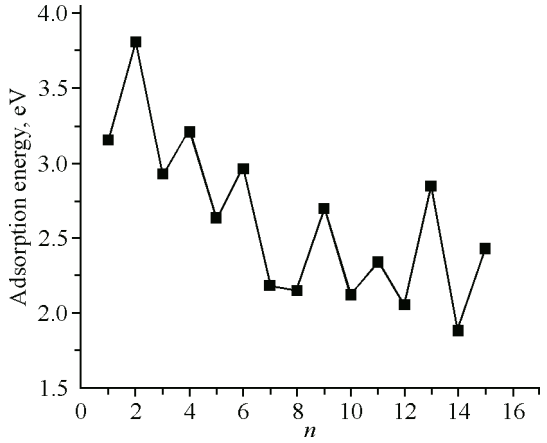

Fig. 4. Adsorption energy of Au loading on the Al_n cluster surface

Al_7Au (2.217 eV), Al_9Au (2.376 eV), $Al_{11}Au$ (2.491 eV), $Al_{13}Au$ (3.306 eV), and $Al_{15}Au$ (2.552 eV) clusters are higher than for the other clusters. Among them, Δ_2E of $Al_{13}Au$ (3.306 eV) is the highest compared with other clusters, which again illustrates that the $Al_{13}Au$ structure is most stable among the Al_nAu clusters. Thus we can conclude that the magic clusters are found at n = 4, 6, 7, 9, 11, 13 for Al_nAu.

We have also calculated the adsorption energy of Au, i.e., the energy released upon Au adsorption by pure aluminum clusters, according to

$$E_{ad} = E[Al_n] + E[Au] - E[Al_nAu]. \quad (4)$$

The calculated values of E_{ad} for the clusters up to $Al_{15}Au$ range between 1.877 eV and 3.806 eV (Fig. 4). The minimum value (1.877 eV) occurs for $Al_{14}Au$, while it takes the maximum value (3.806 eV) for Al_2Au. VEA exhibits an odd-even pattern.

The HOMO—LUMO gap (highest occupied-lowest unoccupied molecular orbital gap) is a useful value to examine the stability of the clusters. It is found that systems with large HOMO—LUMO gaps are, in general, less reactive. In the case of an odd-electron system, we calculate the HOMO—LUMO gap as the smallest spin up-spin down gap. The HOMO—LUMO gaps as thus calculated are presented in Fig. 5. For Al_nAu clusters, local peaks are found at n = 1, 3, 5, 7, 11, 13, implying that the chemical stability of these clusters is higher than that of their neighboring clusters. The magic clusters mostly have a very large HOMO—LUMO gap for the metal clusters. The HOMO—LUMO gap of $Al_{13}Au$ is the highest, except that for Al_1Au. We find a correlation between the HOMO—LUMO gap and the energetic stability of the Al_nAu cluster. We note that the HOMO—LUMO gaps of Al_nAu (except n = 9) present a similar oscillating behavior as observed for the dissociation energy and the second-order energy differences.

Experimentally, the electronic structure is proved via measurements of ionization potentials, electron affinities, polarizabilities, etc. Therefore, we also study these values to understand their evolution with size. These quantities are determined within B3LYP for the lowest-energy structures obtained within the same scheme.

The vertical ionization potential (VIP) is calculated as the self-consistent energy difference between the cluster and its positive ion with the same geometry.

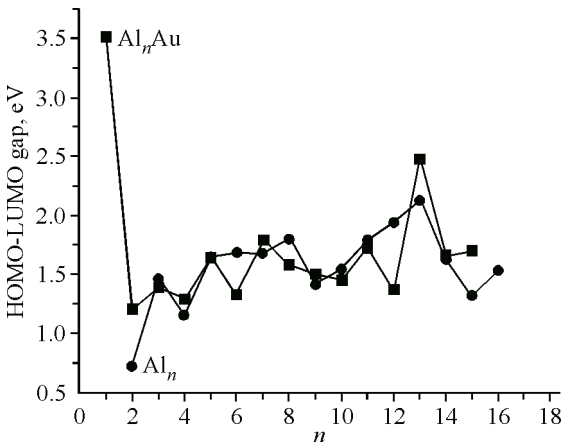

Fig. 5. HOMO—LUMO gap of the Al_nAu and Al_n clusters

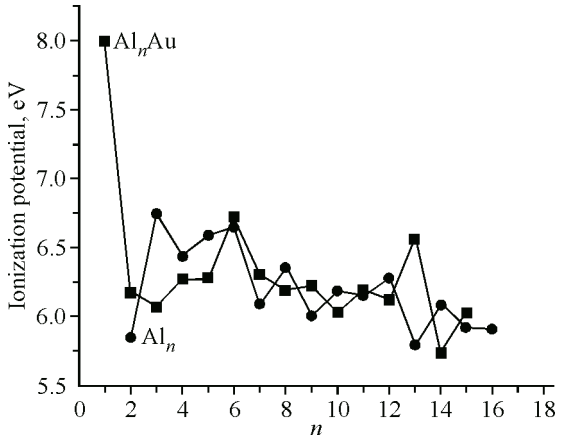

Fig. 6. Ionization potential for Al_nAu and Al_n clusters

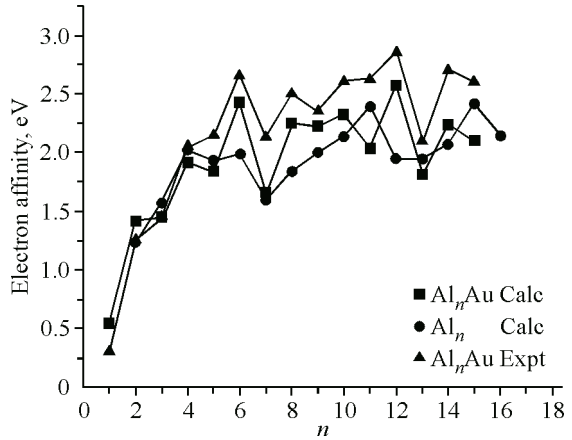

Fig. 7. Calculated and experimentally measured [27] electron affinity for Al_nAu and Al_n clusters

VIP is plotted in Fig. 6 as a function of the cluster size. The corresponding dates are given in Table 1. In general, VIP decreases as the cluster size increases. The peaks occurring at Al_nAu (n = 2, 6, 13) are prominent, with large drops for the following clusters. Also shown in Fig. 6 are VIPs of pure aluminum clusters. These have also been calculated at the B3LYP/genecp level of theory with the structures optimized at the same level of theory.

We have also calculated vertical electron affinities (VEA) for these clusters (Fig. 7 and Table 1) by assuming the geometry for the charged cluster to be the same as for the neutral one. VEA exhibits an odd-even pattern in the whole range, while in pure Al clusters, the odd-even oscillations are not observed. This is again a consequence of the electron pairing effect. In the case of clusters with an even number of valence electrons, the extra electron has to go into the next orbital, which costs energy, resulting in a lower VEA value. It is worth noting that the trend of the theoretical EA values is in accordance with the experimental values [33], which shows that the results of our calculations are reasonable.

Generally, a highly stable cluster has a large gap and VIP and small VEA, implying that it is easier to gain an electron to the complex than to remove an electron from the cluster.
Another useful value is the chemical hardness, which can be approximated as

$$\eta \approx 1/2(I - A) \approx 1/2(\varepsilon_L - \varepsilon_H), \tag{5}$$

where A and I are the electron affinity and the ionization potential, ε_L and ε_H are the HOMO and LUMO energies respectively. Chemical hardness has been established as an electronic quantity that in many cases may be used to characterize the relative stability of a molecule and aggregate through the principle of maximum hardness (PMH) proposed by Pearson [34]. The PMH asserts that molecular systems at equilibrium present the highest hardness value. The hardness of Al_nAu clusters, calculated according to Eq.(5) using VIP for the ionization potential and VEA for the electron affinity, is shown in Fig. 8. Assuming that PMH holds in these systems, we expect the hardness to present an oscillating behavior with local maxima at the clusters with even valence-electron clusters, and the relative energy in Fig. 8 shows that the even valence-electron clusters present higher hardness values than their neighboring clusters from n = 5. We observe the even-odd oscillating feature similar to that

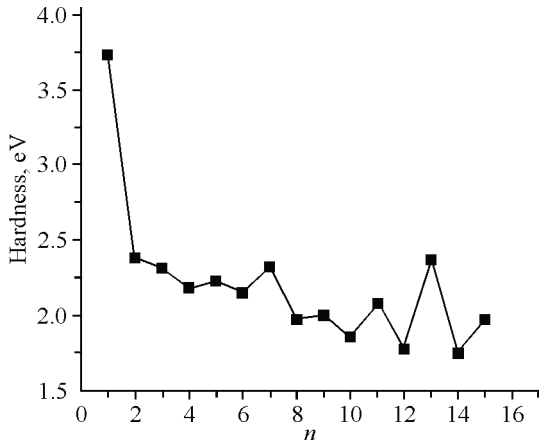

Fig. 8. Hardness of Al_nAu clusters

already stressed in the VIP, VEA, and stability criteria. Stable clusters are harder than their neighboring odd valence-electron systems.

SUMMARY AND CONCLUSIONS

We have performed extensive studies on the growth behavior of Al_nAu (n = 1—15) of the above-mentioned clusters employing density functional calculations. The growth pattern for Al_nAu (n = 1—7, 12, 14, 15) clusters is the Au atom occupying a peripheral position of Al_n clusters. The growth pattern for Al_nAu (n = 8, 10, 13) clusters is Au atoms substituting for Al_{n+1} clusters. It is found that the Au atom substitutes for the surface atom of the Al_{n+1} cluster and occupies a peripheral position. The stability analysis based on the energies and the physical properties clearly shows that the clusters with an even number of valence electrons are more stable than the clusters with an odd number of valence electrons. Especially, the $Al_{13}Au$ is most stable.

This work was financially supported by the National Natural Science Foundation of China (Grant No. 20603021), the Natural Science Foundation of Shanxi (Grant No. 2013011009-6), the High School 131 Leading Talent Project of Shanxi, Undergraduate Training Programs for Innovation and Entrepreneurship of Shanxi Province (Grant No. 2013145), Shanxi Normal University (SD2013CXCY-65, 105088) and Teaching Reform Project of Shanxi Normal University (SD2013JGXM-51).

REFERENCES

1. *Bruma A., Ismail R., Paz-Borbon O. et al.* // Nanoscale. – 2013. – **5**. – P. 646.
2. *Xie S., Tsunoyama H., Kurashige W. et al.* // ACS Catal. – 2012. – **2**. – P. 1519.
3. *Ouyang Y., Wang P., Xiang P. et al.* // Comput., Theoret. Chem. – 2012. – **984**. – P. 68.
4. *Ren X.J., Li B.X.* // Physica B. – 2010. – **405**. – P. 2344.
5. *Wang C.J., Kuang X.Y., Wang H.Q. et al.* // Comput., Theoret. Chem. – 2012. – **980**. – P. 7.
6. *Ma G., Guo L.* // J. Struct. Chem. – 2012. – **53**. – P. 39.
7. *Kumar V., Kawazoe Y.* // Phys. Rev. B. – 2001. – **64**. – P. 115405-1.
8. *Yang P., Ge J.H., Jiang Z.Y.* // J. Mol. Struct.: THEOCHEM. – 2005. – **755**. – P. 75.
9. *Guo L., Wu H.S.* // Eur. Phys. J. D. – 2007. – **42**. – P. 259.
10. *Venkataramanan N.S., Suvitha A., Note R. et al.* // J. Mol. Struct.: THEOCHEM. – 2009. – **902**. – P. 72.
11. *Belcher D.R., Randy M.W., King B.V.* // Mater. Transact. – 2007. – **48**. – P. 689.
12. *Zope R.R., Baruah T.* // J. Phys. Rev. A. – 2001. – **64**. – P. 053202-1.
13. *Majumder C., Kandalam A.K., Jena P.* // Phys. Rev. B. – 2006. – **74**. – P. 205437-1.
14. *Kimble M.L., Castleman A.W. Jr et al.* // Collect. Czech. Chem. Commun. – 2007. – **72**. – P. 185.
15. *Pittaway F., Paz-Borbón L.O., Johnston R.L. et al.* // J. Phys. Chem. C. – 2009. – **113**. – P. 9141.
16. *Li Y.F., Kuang X.Y., Wang S.J. et al.* // J. Phys. Chem. A. – 2010. – **114**. – P. 11691.
17. *Manbeck G.F., Brennessel W.W., Stockland R.A. et al.* // J. Amer. Chem. Soc. – 2010. – **132**. – P. 12307.
18. *Die D., Kuang X.Y., Zhu B. et al.* // Physica B. – 2011. – **406**. – P. 3160.
19. *Cheng L., Kuang X.Y., Lu Z.W. et al.* // J. Phys. Chem. A. – 2011. – **115**. – P. 9273.
20. *Zhao G.F., Wang Y.L., Sun J.M. et al.* // Acta Phys.-Chim. Sin. – 2012. – **28**. – P. 1355.
21. *Wang C.J., Kuang X.Y., Wang H.Q. et al.* // Comput., Theoret. Chem. – 2012. – **1002**. – P. 31.
22. *Knight W.D., Clemenger K., de Heer W.A. et al.* // Phys. Rev. Lett. – 1984. – **52**. – P. 2141.
23. *Brack M.* // Rev. Mod. Phys. – 1993. – **65**. – P. 677.
24. *Frisch M.J., Trucks G.W., Schlegel H.B. et al.* Gaussian, Inc. Pittsburgh, PA, 2003.
25. *Becke A.D.* Densityfunctional thermochemistry. III // J. Chem. Phys. – 1993. – **98**. – P. 5648-1.
26. *Hay P.J., Wadt W.R.* // J. Chem. Phys. – 1985. – **82**. – P. 270.
27. *Wadt W.R., Hay P.J.* // J. Chem. Phys. – 1985. – **82**. – P. 284.
28. *Hay P.J., Wadt W.R.* // J. Chem. Phys. – 1985. – **82**. – P. 299.
29. *Chuang F.C., Wang C.Z., Ho K.H.* // Phys. Rev. B. – 2006. – **73**. – P. 125431.
30. *Negishi Y., Nakamura Y., Nakajima A. et al.* // J. Chem. Phys. – 2001. – **115**. – P. 3657.
31. *Rosen B.* Spectroscopic Data Relative to Diatomic Molecules. – New York: Oxford University Press, 1970.
32. *Gingerich K.A., Blue G.D.* // J. Chem. Phys. – 1973. – **59**. – P. 185.
33. *Götz M.* – 2010. – URN: http: // nbn-resolving.de/urn:nbn:de:bsz:352-opus-122974.
34. *Pearson R.G.* Chemical Hardness: Applications from Molecules to Solids. – Weinheim: Wiley-VCH, 1997.